International Journal of Mechanical, Industrial and Aerospace Sciences
ISSN: 2517-9950
Vol:7, No:6, 2013

Acoustic Analysis with Consideration of Damping Effects of Air Viscosity in Sound Pathway

M. Sasajima, M. Watanabe, T. Yamaguchi, Y. Kurosawa, and Y. Koike

***Abstract*—**Sound pathways in the enclosures of small earphones are very narrow. In such narrow pathways, the speed of sound propagation and the phase of sound waves change because of the air viscosity. We have developed a new finite element method that includes the effects of damping due to air viscosity for modeling the sound pathway. This method is developed as an extension of the existing finite element method for porous sound-absorbing materials. The numerical calculation results using the proposed finite element method are validated against the existing calculation methods.

***Keywords*—** Simulation, FEM, air viscosity, damping.

I. Introduction

With the many advancements in the performance of computers, CAE (Computer Aided Engineering) has been used extensively in recent years for acoustic analyses. However, the conventional analysis approach is still being predominantly used for relatively large structures or large equipment. For example, for a structure with a small volume of a few cubic centimeters, such as an earphone enclosure, very few methods of sound propagation analyses are available. In small earphones, enclosures are divided into several compartments, and the sound pathways connecting these rooms are often very narrow. The viscosity of air in these narrow pathways results in damping. Consequently, the speed of sound propagation decreases, and a phase delay occurs. Therefore, to carry out accurate acoustic analysis, we need to consider the effects of the "damping due to air viscosity" which are not considered in a conventional acoustic analysis.

In this study, we have developed a new finite element method that includes the effects of the damping due to air viscosity in narrow places in the sound pathway. This has been developed as an extension of the acoustic finite element method proposed by Yamaguchi [1], [2] for a porous sound-absorbing material [3]. Moreover, we attempted numerical analysis in the frequency domain with our acoustic solver that uses the proposed finite element method. For the numerical calculations, we used a tube model having a circular cross section. Then, we compared the proposed finite element method with the theoretical analysis, and with the generally used finite element analysis that does not include the effects of the viscosity of the air.

M. Sasajima, M. Watanabe, and Y. Koike are with the Strategic Research & Development Division, Foster electric Co., Ltd., 196-8550, 1-1-109 Tsutsujigaoka, Akishima, Tokyo, Japan (phone: 042-847-3334; e-mail: sasajima@ foster.co.jp, mtwatanabe@ foster.co.jp, koike@ foster.co.jp).

T. Yamaguchi is with the Department of Mechanical System Engineering, Gunma University, 376-8515, 1-5-1, Tenjin-cho, Kiryu, Gunma, Japan (e-mail: yamagme3@gunma-u.ac.jp).

Y. Kurosawa is with the Department of Precision Mechanical System Engineering, Teikyo University, 320-8551, 1-1, Toyosatodai, Utsunomiya, Tochigi, Japan (e-mail: ykurosawa@mps.teikyo-u.ac.jp).

II. Numerical Procedures

We have developed a new finite element method that incorporates the air viscosity at small amplitudes. Fig. 1 shows the direct Cartesian coordinate system and a constant strain element of a three-dimensional tetrahedral. Here, u_x, u_y, and u_z are the displacements in the x, y, and z directions at arbitrary points in the element.

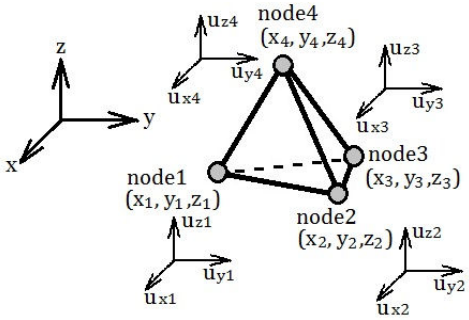

Fig. 1 Direct Cartesian coordinate system and a constant strain element

The strain energy $\widetilde{U}$ can be expressed as follows:

$$\widetilde{U} = \frac{1}{2} E \iiint_e \left(\frac{\partial u_x}{\partial x} + \frac{\partial u_y}{\partial y} + \frac{\partial u_z}{\partial z} \right)^2 dxdydz \qquad (1)$$

where E is the bulk modulus of elasticity of the medium, air. The time derivative of the particle displacement is expressed as $\dot{u}$. Therefore, the kinetic energy $\widetilde{T}$ can be expressed as follows:

$$\widetilde{T} = \frac{1}{2} \iiint_e \rho \{\dot{u}\}^T \{\dot{u}\} dxdydz \qquad (2)$$

where ρ is the effective density of the element. T represents a transpose. The viscosity energy $\widetilde{D}$ of a viscous fluid can be expressed as follows:

$$\widetilde{D} = \iiint_e \frac{1}{2}\{\overline{T}\}^T \{\Gamma\} dxdydz \tag{3}$$

where $\{\overline{T}\}$ is the stress vector attributable to viscosity. The relationship between the particle velocity and the stress can be expressed as follows:

$$\{\overline{T}\} \equiv \begin{Bmatrix} \tau_{xx} \\ \tau_{yy} \\ \tau_{zz} \\ \tau_{xy} \\ \tau_{yz} \\ \tau_{zx} \end{Bmatrix} = \begin{bmatrix} \frac{4}{3}\mu\frac{\partial}{\partial x} & -\frac{2}{3}\mu\frac{\partial}{\partial y} & -\frac{2}{3}\mu\frac{\partial}{\partial z} \\ -\frac{2}{3}\mu\frac{\partial}{\partial x} & \frac{4}{3}\mu\frac{\partial}{\partial y} & -\frac{2}{3}\mu\frac{\partial}{\partial z} \\ -\frac{2}{3}\mu\frac{\partial}{\partial x} & -\frac{2}{3}\mu\frac{\partial}{\partial y} & \frac{4}{3}\mu\frac{\partial}{\partial z} \\ \mu\frac{\partial}{\partial y} & \mu\frac{\partial}{\partial x} & 0 \\ 0 & \mu\frac{\partial}{\partial z} & \mu\frac{\partial}{\partial y} \\ \mu\frac{\partial}{\partial z} & 0 & \mu\frac{\partial}{\partial x} \end{bmatrix} \begin{Bmatrix} \dot{u}_x \\ \dot{u}_y \\ \dot{u}_z \end{Bmatrix} \tag{4}$$

where $\dot{u}_x$, $\dot{u}_y$, and $\dot{u}_z$ are the particle velocities in the x, y, and z directions at arbitrary points in the element, and μ is the coefficient of viscosity of the medium. In the above equation, $\{\Gamma\}$ is the strain vector. The relationship between the particle velocity and the strain can be expressed by the constant strain element of a three-dimensional tetrahedral, as shown in Fig. 2.

$$\{\Gamma\} \equiv \begin{Bmatrix} \gamma_{xx} \\ \gamma_{yy} \\ \gamma_{zz} \\ \gamma_{xy} \\ \gamma_{yz} \\ \gamma_{zx} \end{Bmatrix} = \frac{1}{6V_e} \begin{bmatrix} b_1 & 0 & 0 & b_2 & 0 & 0 & b_3 & 0 & 0 & b_4 & 0 & 0 \\ 0 & c_1 & 0 & 0 & c_2 & 0 & 0 & c_3 & 0 & 0 & c_4 & 0 \\ 0 & 0 & d_1 & 0 & 0 & d_2 & 0 & 0 & d_3 & 0 & 0 & d_4 \\ c_1 & b_1 & 0 & c_2 & b_2 & 0 & c_3 & b_3 & 0 & c_4 & b_4 & 0 \\ 0 & d_1 & c_1 & 0 & d_2 & c_2 & 0 & d_3 & c_3 & 0 & d_4 & c_4 \\ d_1 & 0 & b_1 & d_2 & 0 & b_2 & d_3 & 0 & b_3 & d_4 & 0 & b_4 \end{bmatrix} \begin{Bmatrix} \dot{u}_{x1} \\ \dot{u}_{y1} \\ \dot{u}_{z1} \\ \dot{u}_{x2} \\ \dot{u}_{y2} \\ \dot{u}_{z2} \\ \dot{u}_{x3} \\ \dot{u}_{y3} \\ \dot{u}_{z3} \\ \dot{u}_{x4} \\ \dot{u}_{y4} \\ \dot{u}_{z4} \end{Bmatrix} \tag{5}$$

V_e is the volume of the element and b_1-d_4 are constants. These constants can be expressed as follows:

$$\left.\begin{aligned} b_k &= \tilde{\varepsilon}_k \{y_l(z_n - z_m) + y_m(z_l - z_n) + y_n(z_m - z_l)\} \\ c_k &= \tilde{\varepsilon}_k \{z_l(x_n - x_m) + z_m(x_l - x_n) + z_n(x_m - x_l)\} \\ d_k &= \tilde{\varepsilon}_k \{x_l(y_n - y_m) + x_m(y_l - y_n) + x_n(y_m - y_l)\} \\ \tilde{\varepsilon}_k &= \begin{cases} 1 & (k = 1,3) \\ -1 & (k = 2,4) \end{cases} \end{aligned}\right\} \tag{6}$$

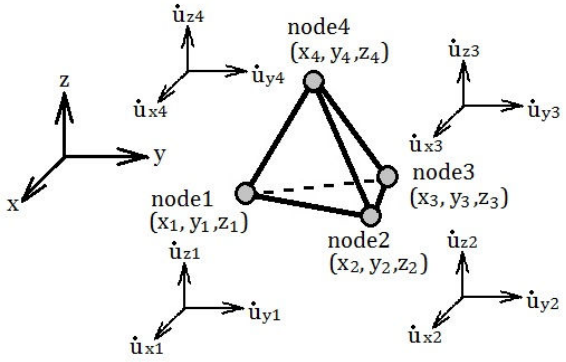

Fig. 2 Relationship between particle velocity and strain

where subscripts *k, l, m*, and *n* represent the circular rotation of 1, 2, 3, and 4. Next, we consider the formulation of the motion equation of an element, for the acoustic analysis model that considers viscous damping. The potential energy $\widetilde{V}$ can be expressed as follows:

$$\widetilde{V} = \int_\Gamma \{u\}^T \{\overline{P}\} d\Gamma + \iiint_e \{u\}^T \{F\} dxdydz \tag{7}$$

where $\{\overline{P}\}$ is the surface force vector. $\{F\}$ is the body force vector. And $\int_\Gamma d\Gamma$ represents the integral of the element boundary. The total energy $\widetilde{E}$ can be derived by using the following expression:

$$\widetilde{E} = \widetilde{U} + \widetilde{D} - \widetilde{T} - \widetilde{V} \tag{8}$$

We can obtain the following discretized equation of an element by using Lagrange's equations:

$$\frac{d}{dt}\frac{\partial \widetilde{T}}{\partial \dot{u}_{ei}} - \frac{\partial \widetilde{T}}{\partial u_{ei}} + \frac{\partial \widetilde{U}}{\partial u_{ei}} - \frac{\partial \widetilde{V}}{\partial u_{ei}} + \frac{\partial \widetilde{D}}{\partial u_{ei}} = 0 \tag{9}$$

where u_{ei} is the *i-th* component of the nodal displacement vector $\{u_e\}$ and $\dot{u}_{ei}$ is the *i-th* component of the nodal particle velocity vector $\{\dot{u}_e\}$. We can obtain the following discretized equation of an element by substituting (1)–(7) in (9):

$$-\omega^2[M_e]\{u_e\} + [K_e]\{u_e\} + j\omega[C_e]\{u_e\} = \{f_e\} \tag{10}$$

We use $\{\dot{u}_e\} = j\omega\{u_e\}$ in this equation because a periodic motion having angular frequency ω is assumed. $[M_e]$, $[K_e]$, $[C_e]$ and $\{f\}_e$ are the element mass matrix, element stiffness matrix, element viscosity matrix, and nodal force vector, respectively.

III. Expressions for Damping in Porous Materials

In the motion equation (10), we use the following model having a complex effective density, and a complex bulk modulus of elasticity in the element stiffness matrix $[K_e]$, and the element mass matrix $[M_e]$ [1]–[4].

$$\rho \Rightarrow \rho^* = \rho_R + j\rho_I \tag{11}$$

$$E \Rightarrow E^* = E_R + jE_I \tag{12}$$

where j denotes the imaginary component. Note that ρ_R and ρ_I are the real and imaginary parts of ρ^*, respectively. Here ρ_R is the density of air inside the porous sound-absorbing material and ρ_I is related to the flow resistance of air inside the sound-absorbing material. We consider the resistance to the air flow at a high frequency by using the complex density. The variables E_R and E_I are the real and imaginary parts of E^*, respectively and E_I is related to the hysteresis between the sound pressure and the volume strain. The dissipated energy due to E_I is converted into heat energy corresponding to the enclosed area of the hysteresis curve obtained in one cycle; this is known as the attenuation effect.

As a result, the equations of the sound field in the element that includes damping are formulated using complex linear simultaneous equations.

$$-\omega^2([M_e]_R + j[M_e]_I)\{u_e\} + ([K_e]_R + j[K_e]_I)\{u_e\} + j\omega[C_e]\{u_e\} = \{f_e\} \tag{13}$$

where $[K_e]_R$ and $[K_e]_I$ are the real and imaginary parts of $[K_e]$, respectively and $[M_e]_R$ and $[M_e]_I$ are the real and imaginary parts of $[M_e]$, respectively. All nodal particle displacements can be calculated by solving (13) for the particle displacement. Furthermore, the strain and the sound pressure of each element can be calculated from the nodal particle displacements.

IV. Calculation

A. Damping Analysis by the Three Dimensional Finite Element Method

To verify our method, we carried out an acoustic damping analysis for tubes using three-dimensional finite elements model. When we made this model, we use HyperMesh v11.0 (Altair Engineering Inc.) at meshing. As shown in Fig. 3, this model is 1/4 solid model symmetrical about x-z plane and x-y plane. And the air inside the tube is modeled using three-dimensional tetrahedral elements having four nodes. The number of divided elements was 33 in the axial direction, and 10 in the radial direction. Both ends of the tube were closed. The radius of model was 0.5 mm. The length of the tube was 16.6 mm.

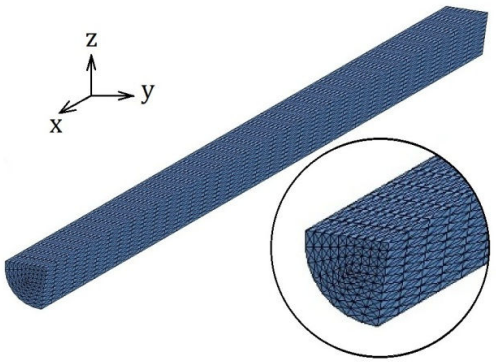

Fig. 3 Three-dimensional tube for finite element method

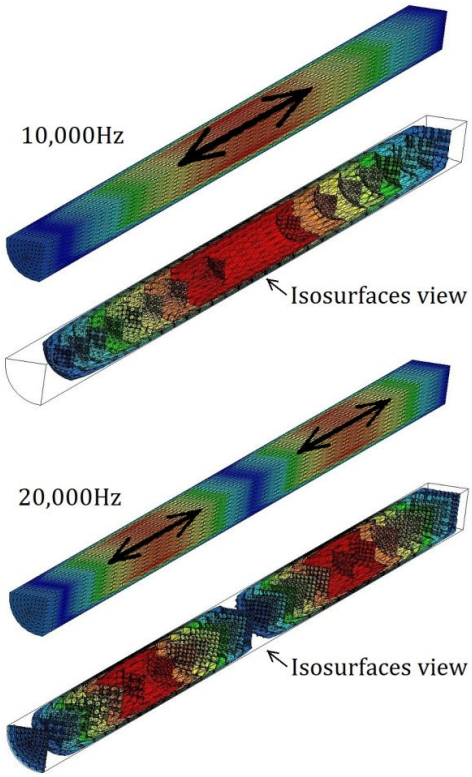

Fig. 4 The distribution of particle displacements contour and the isosurface view

We selected the effective density ρ_R = 1.2 kg/m^3, coefficient of viscosity μ = 1.82 × 10^{-5} N•s/m^2, real part of the complex volume elasticity E_R = 1.4 × 10^5 Pa, and sound propagation speed c = 340 m/s for air. As the boundary conditions, the particle displacements of all nodes on the outside in contact with the tube were fixed, except for the plane of symmetry.

Fig. 4 shows the contours of the calculated particle displacements and the isosurface view of the model tube for the proposed finite element method, near the resonance conditions (10,000 Hz and 20,000 Hz). As can be seen, the magnitude of the displacement of the particles changes significantly near the outside of the tube. However, the displacement is flat close to the center of the tube.

B. Damping Analysis by Theoretical Analysis

We have carried out theoretical analysis of the resonant response of the tube for comparison and verification of the proposed finite element method. We consider a straight duct with circular cross section. In this case, the frequency response of the pressure can be expressed by the following general expression,

$$P = -j\rho c v_0 e^{j\omega t} \frac{\cos k(x-l)}{\sin kl} \tag{14}$$

where ρ is density of the air, c is the speed of sound, l is the length of the tube, x is a position of reference point, k is ω/c. v_0 is an excitation velocity, and t is time.

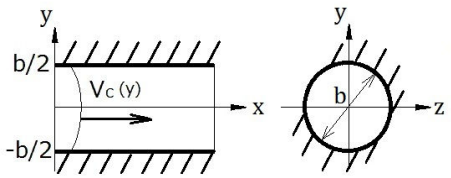

Fig. 5 Three-dimensional tube model and velocity $Vc_{(y)}$

In this equation, we introduce the complex sound speed c^* and the complex effective density ρ_c^* to include the attenuation due to the viscosity of the air. We replace the speed of sound and the density with the complex sound speed and the complex effective density as shown below.

$$\rho \Rightarrow \rho_c^* \tag{15}$$

$$c \Rightarrow c^* \tag{16}$$

Using the two substitutions above in equitation (14) and using the notation of Craggs and Hildebrant [5], the effective density can be written as

$$\rho_c^* \equiv \rho_0 + \frac{R_c}{j\omega} \tag{17}$$

where ρ_0 is mass density, and R_c is flow resistance. The real part of the complex effective density ρ_c^* is the density of the air related to the inertial force. Imaginary part is a term that represents the viscous resistance or resistance to flow. In addition, the flow resistance per unit area R_c in the high frequency region can be expressed as follows, using the capillary flow theory [6].

$$R_c = \frac{12\mu}{b^2} \frac{\frac{1}{3} k_1 j^{\frac{1}{2}} \tanh\left(k_1 j^{\frac{1}{2}}\right)}{1 - \left(\frac{1}{k_1 j^{\frac{1}{2}}}\right) \tanh\left(k_1 j^{\frac{1}{2}}\right)} \tag{18}$$

where b is the diameter of the circular cross section tube. And k_1 is expressed as follows:

$$k_1 = \frac{b}{2}\sqrt{\frac{\rho_0 \omega}{\mu}} \tag{19}$$

$$c^* = \sqrt{\frac{\kappa}{\rho_c^*}} = \sqrt{\frac{\gamma p_0}{\rho_c^*}} \tag{20}$$

where κ is the bulk modulus, p_0 is atmospheric pressure and γis the specific heat at constant volume. For the case of the 0.25 mm radius tube, the complex density and complex sound velocity are shown in Figs. 6 and 7 respectively.

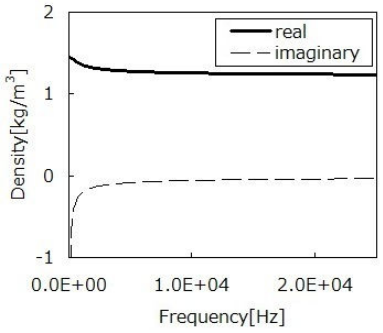

Fig. 6 Density trend for the three-dimensional tube model

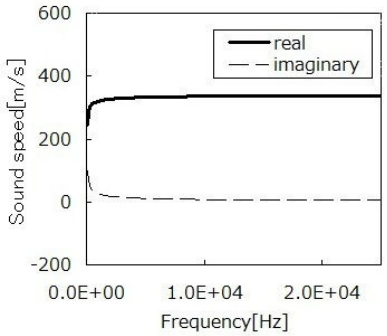

Fig. 7 Velocity trend for the three-dimensional tube model

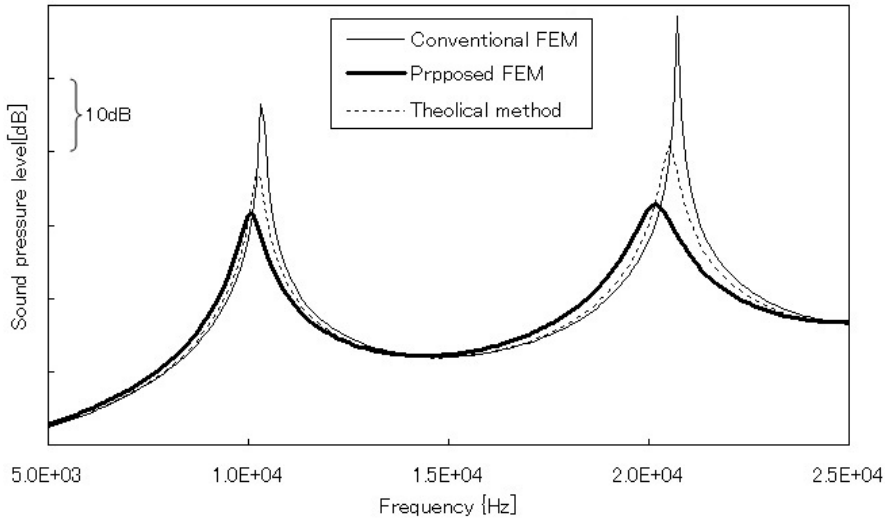

Fig. 8 Pressure versus frequency response for a three-dimensional tube model (Diameter is 0.5 mm for the model tube)

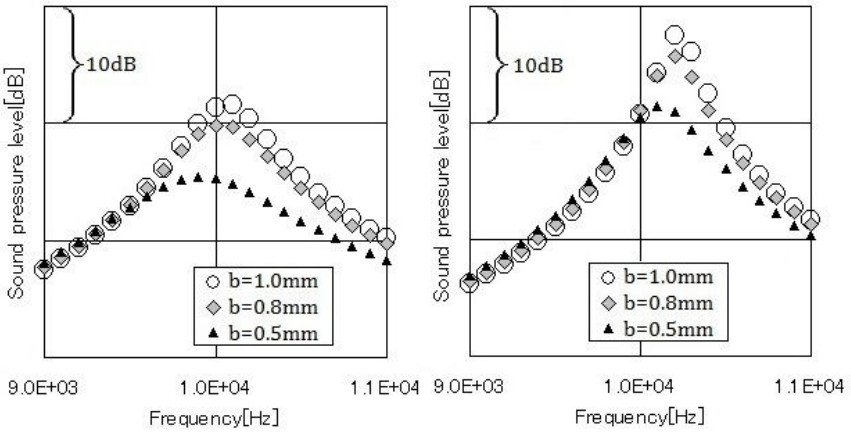

(a) Proposed FEM (b) Theoretical method

Fig.9 Effect of diameters compared between Proposed FEM and Theoretical method at 10,000Hz

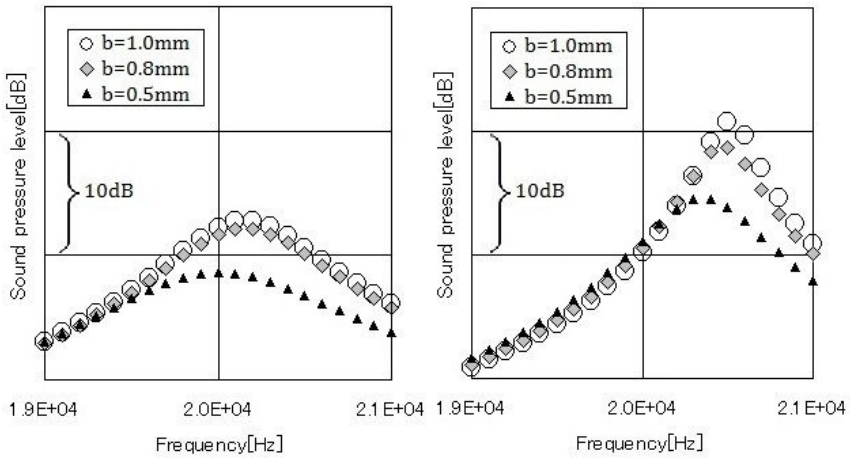

(a) Proposed FEM (b) Theoretical method

Fig.10 Effect of diameters compared between Proposed FEM and Theoretical method at 20,000Hz

By calculating the frequency response of (13) using the values of these parameters, the theoretical solution that includes the viscosity is obtained.

C. Verification and Comparison of the Proposed Method

We have analyzed frequency responses of the proposed finite element method (Proposed FEM), and compared it with the above described theoretical method (Theoretical method) that includes the viscosity, and with the conventional acoustic finite element method (Conventional FEM) that does not include the attenuation. Fig. 8 shows the comparison of the analysis results for a model tube of radius 0.5 mm. The condition of excitation was the constant displacement excitation. From Fig. 8, we determined the effect of damping on the calculated results by using the proposed FEM and the theoretical method cases. The conventional FEM does not show attenuation for the resonance peaks.

In addition, we analyzed the resonant responses with different tube diameters using both the proposed FEM and the theoretical method cases. Fig. 9 shows the effect of diameters of circular tube models on the response, for the proposed FEM and the theoretical method cases at around 10,000Hz. And Fig. 10 shows the effect of diameters of circular tube models on the response at around 20,000Hz. The diameter b of the circular tubes were 0.5 mm, 0.8 mm, and 1.0 mm. The condition of excitation was the constant displacement excitation. As can be seen from Fig.9 and Fig.10, when the tube diameter is narrow, the resonance peak decrease because flow resistance increases. This trend is the same for both methods.

A comparison of the results of the proposed method with that of the theoretical method shows that the proposed method shows slightly larger attenuation. We think this is coming due to the influence of the mesh size and order near the boundary layer. As a result of the first order elements used in this analysis, the mesh size was somewhat larger near boundary layer that had large change of displacement.

V. Conclusion

We have developed a new acoustic finite element method that considers the effects of damping by the viscosity of air. We compared calculation results of sound pressure versus frequency characteristics using the proposed method with that of the theoretical method, and the conventional acoustic finite element method without viscosity of air.

The comparison shows that the general shapes of the characteristics are very close. For future, we are planning to extend this research further, to fully understand the damping effects of air on sound waves. Thereby, we hope to establish a technology that allows consideration early in the design stage, and to provide excellent sound solutions.

References

[1] T. Yamaguchi, J. Tsugawa, H. Enomoto and Y. Kurosawa, "Layout of Sound Absorbing Materials in 3D Rooms Using Damping Contributions with Eigenvectors as Weight Coefficients", Journal of System Design and Dynamics, Vol. 4-1, pp. 166-176, 2010.

[2] T. Yamaguchi, Y. Kurosawa and H. Enomoto, "Damped Vibration Analysis Using Finite Element Method with Approximated Modal Damping for Automotive Double Walls with a Porous Material", Journal of Sound and Vibration, Vol. 325, pp. 436-450, 2009.

[3] M. Sasajima, T. Yamaguchi and A. Hara, "Acoustic Analysis Using Finite Element Method Considering Effects of Damping Caused by Air Viscosity in Audio Equipment", Applied Mechanics and Materials, Vol. 36, pp. 282-286, 2010.

[4] H. Utsuno, T. Tanaka, Y. Morisawa and T. Yoshimura, "Prediction of Normal Sound Absorption Coefficient for Multi-Layer Sound Absorbing Materials by Using the Boundary Element Method", Transactions of Japan Society of Mechanical Engineers, Vol. 56-532C, pp. 3248-3252, 1990.

[5] A. Craggs and J.G.Hildebrandt, "Effective densities and resistivities for acoustic propagation in narrow tubes", Journal of Sound and Vibration, Vol.92, pp321-331, 1984.

[6] M. A. Biot, "Theory of Propagation of Elastic Waves in a Fluid-Saturated Porous Solid. Ⅱ. Higher Frequency Range", Journal of the Acoustical Society of America, Vol.28, pp179-191, 1956.